SANDIA REPORT
SAND2005-1700
Unlimited Release
Printed March 2005

# Toxin Studies Using an Integrated Biophysical and Structural Biology Approach

Andrea L. Slade[†], Anne E. Schroeder[†], Julie A. Last[†], Joseph S. Schoeniger[‡], Christopher M. Yip[§], and Darryl Y. Sasaki[†]

Prepared by

Sandia National Laboratories

Albuquerque, New Mexico 87185 and Livermore, California 94550

Sandia is a multiprogram laboratory operated by Sandia Corporation,

a Lockheed Martin Company, for the United States Department of Energy's National Nuclear Security Administration under Contract DE-AC04-94-AL85000.



Sandia National Laboratories

Issued by Sandia National Laboratories, operated for the United States Department of Energy by Sandia Corporation.



Available to DOE and DOE contractors from
U.S. Department of Energy
Office of Scientific and Technical Information
P.O. Box 62
Oak Ridge, TN 37831

Telephone: (865) 576-8401
Facsimile: (865) 576-5728
E-Mail: reports@adonis.osti.gov
Online ordering: http://www.doe.gov/bridge

Available to the public from
U.S. Department of Commerce
National Technical Information Service
5285 Port Royal Rd
Springfield, VA 22161

Telephone: (800) 553-6847
Facsimile: (703) 605-6900
E-Mail: orders@ntis.fedworld.gov
Online order: http://www.ntis.gov/help/ordermethods.asp?loc=7-4-0#online

SAND2005-1700
Unlimited Release
Printed March 2005

# Toxin Studies Using an Integrated Biophysical and Structural Biology Approach

**Andrea L. Slade[†], Anne E. Schroeder[†], Julie A. Last[†], Joseph S. Schoeniger[‡], Christopher M. Yip[§], and Darryl Y. Sasaki[†]**

Sandia National Laboratories
[†]Biomolecular Materials and Interfaces Dept., Albuquerque, NM 87185
[‡]Biosystems Research Dept., Livermore, CA 94551

[§]University of Toronto
Dept. of Biochemistry
Dept. of Chemical Engineering & Applied Chemistry
Institute of Biomaterials and Biomedical Engineering
Toronto, Ontario M5S 3G9
CANADA

## Abstract

Clostridial neurotoxins, such as botulinum and tetanus, are generally thought to invade neural cells through a process of high affinity binding mediated by gangliosides, internalization via endosome formation, and subsequent membrane penetration of the catalytic domain activated by a pH drop in the endosome.[i,ii] This surface recognition and internalization process is still not well understood with regard to what specific membrane features the toxins target, the intermolecular interactions between bound toxins, and the molecular conformational changes that occur as a result of pH lowering. In an effort to elucidate the mechanism of tetanus toxin binding and permeation through the membrane a simple yet representative model was developed that consisted of the ganglioside $G_{T1b}$ incorporated in a bilayer of cholesterol and DPPC (dipalmitoylphosphatidyl choline). The bilayers were stable over time yet sensitive towards the binding and activity of whole toxin. A liposome leakage study at constant pH as well as with a pH gradient, to mimic the processes of the endosome, was used to elucidate the effect of pH on the toxin's membrane binding and permeation capability. Topographic imaging of the membrane surface, via *in situ* tapping mode AFM, provided nanoscale characterization of the toxin's binding location and pore formation activity.

This page intentionally left blank

# Table of Contents

**Abstract** ..... **3**

**Table of Contents** ..... **5**

**Table of Figures** ..... **6**

**Background** ..... **7**

Liposome Leakage Studies ..... 8
Scanning Probe Imaging of the C Fragment on Lipid Membrane ..... 13

Conclusion ..... 18
Experimental ..... 19

Liposome leakage studies ..... 19
*In situ* Tapping Mode Atomic Force Microscopy ..... 20

**References** ..... **21**

# Table of Figures

Figure 1. (a) The two-chain structure of TetTx. (b) The 3D structure of Tet C. ..... 7

Figure 2. Mechanism of tetanus toxin internalization and activation in a neuronal cell. .. 8

Figure 3. Model of the lipid membrane of a cell and a cut away view of a lipid bilayer vesicle, or liposome. ..... 9

Figure 4. Illustrated model of the liposome leakage study where toxin binding and pore formation leads to dye leakage and a subsequent increase in dye fluorescence. ..... 9

Figure 5. Lipids used in the leakage study: $G_{T1b}$, DPPC, and cholesterol. ..... 10

Figure 6. Plot of fluorescence intensity of Texas red (excitation at 586 nm, emission monitored at 620 nm) as it leaks out of the control and $G_{T1b}$ containing liposomes at pH 7 and 4 and with the pH gradient from 7 to 4. ..... 11

Figure 7. Leakage of Texas red from 50% DPPC/cholesterol liposomes in the presence of tetanus toxin at constant pH of 7 and 4 and with the pH gradient from 7 to 4..... 12

Figure 8. Leakage of Texas red from 5% $G_{T1b}$/47.5% DPPC/47.5% cholesterol liposomes in the presence of tetanus toxin at constant pH of 7 and 4 and at with the pH gradient from 7 to 4..... 13

Figure 9. AFM image of tetanus toxin C fragment on mica (left) and structural models prepared using the PDB model 1FV2 and the SwissPDB Viewer software package..... 14

Figure 11. Illustration of the DPOPC/DPPC supported lipid bilayer and the vesicle fusion process on mica in the solution cell of the AFM. ..... 15

Figure 12. AFM images with height profiles of the 10% $G_{T1b}$/45% DPOPC/45% DPPC bilayers on mica (a) before and (b) after ~2 hours and then (c – e) after ~12 hours of incubation with Tet C..... 16

Figure 13. 3D AFM image with of the 10% $G_{T1b}$/45% DPOPC/45% DPPC bilayers on mica following 12h incubation with tetanus toxin C fragment at pH 7..... 17

Figure 14. AFM image with of the 10% $G_{T1b}$/45% DPOPC/45% DPPC bilayers on mica following 12h incubation with tetanus toxin C fragment at pH 4..... 18

# Background

Tetanus toxin (TetTx) is a 150 kDa protein produced by *Clostridium tetani* and is composed of two disulfide-linked chains: the light chain (50kDa) and the heavy chain (100 kDa) (Figure 1).[iii,iv] Although it has been known for years that TetTx is the agent responsible for spasticity and convulsions associated with human tetanus by blocking the release of inhibitory neurotransmitters in the central nervous system,[v] the mode of action of TetTx at the molecular level still remains fairly elusive.

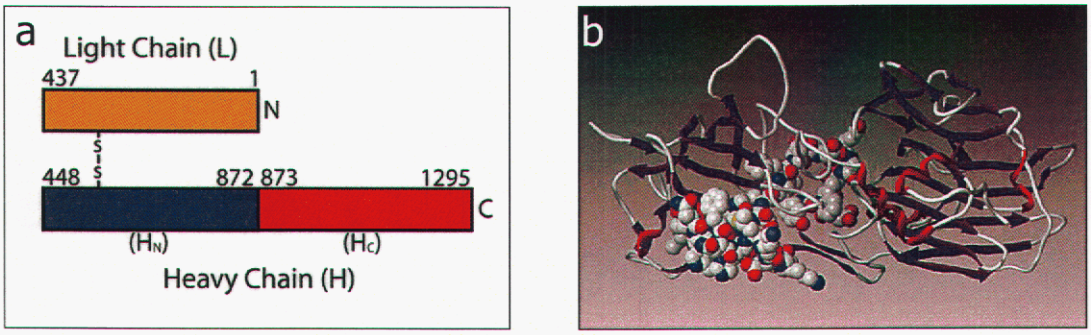


**Figure 1. (a) The two-chain structure of TetTx. (b) The 3D structure of Tet C. The last 34 residues of Tet C (shown as spacefill) are involved in ganglioside recognition. The image was prepared using the PDB model 1FV2 and the Sybyl molecular graphics software package (Tripos Inc.).**

Binding of TetTx to its ganglioside membrane receptor, trisialoganglioside $G_{T1b}$, in neuronal cells is facilitated by the 50 kDa C-terminal region of the heavy chain, known as the C-fragment.[vi] Once bound to the membrane surface, the toxin is taken into the cell by endocytosis. It is proposed that the pH inside the endosome, which changes from neutral to acidic during protein digestion, triggers a conformational change in the toxin that increases the hydrophobicity of the molecule facilitating its insertion into the endosomal membrane.[vii,viii] The toxin has been shown to be capable of forming pores in lipid bilayers at acidic pH.[ix] It is believed that the catalytic light chain (L-chain) is then translocated into the cell's cytosol through these pores. Once in the cytosol, the L-chain specifically cleaves the synaptic SNARE protein synaptobrevin, thereby preventing fusion of neurotransmitter secretory vesicles to the nerve terminal membrane, and thus blocking the release of inhibitory neurotransmitters. The complete process is shown in Figure 2.

Our goal was to study the membrane recognition and permeation of TetTx on the cell membrane at the molecular level to enable means of inhibiting Clostridial neurotoxin lethality. A model membrane system was required that would allow an accurate analysis of the toxin's binding orientation, supramolecular organization on the membrane surface with other bound toxin molecules, and conformational changes associated with pore formation.

## Liposome Leakage Studies

Cell membranes are a complex mixture of lipids, steroidal molecules, proteins, and gangliosides that can create complex topologies and physical interactions in the membrane (Figure 3a). A simple form of a cell membrane is the lipid bilayer vesicle, or liposome.[x] The liposome can be prepared as a multilamellar or single lamellar structure, as shown in Figure 3b, that has an inner aqueous phase that is separated from the exterior bulk aqueous solution by the lipid membrane. This architecture provides an excellent means to evaluate the pore forming activity of the toxin on various lipid membrane compositions by monitoring the leakage of the liposome's contents. Fluorophores can be entrapped at a high concentration within the liposome leading to low solution fluorescence due to self-quenching. Pore formation in the liposomal membrane releases the dye to the bulk solution reducing self-quenching of the dye and subsequent increase in dye fluorescence. A schematic of this process is shown in Figure 4.

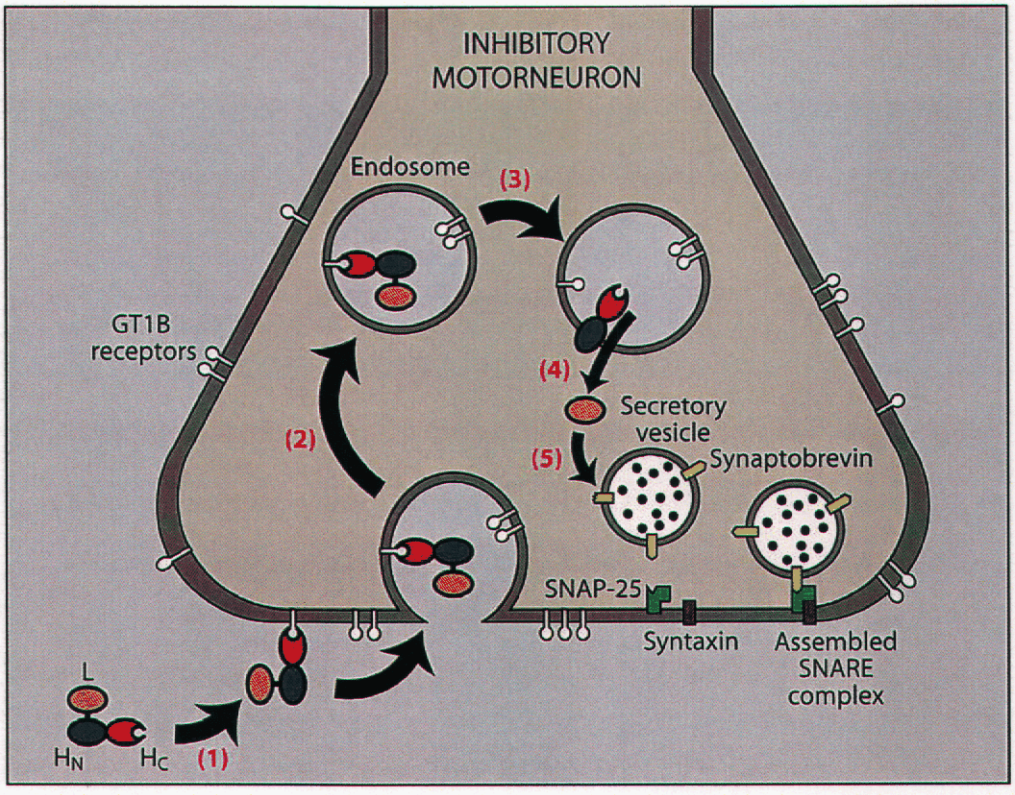


**Figure 2. Mechanism of tetanus toxin internalization and activation in a neuronal cell.**

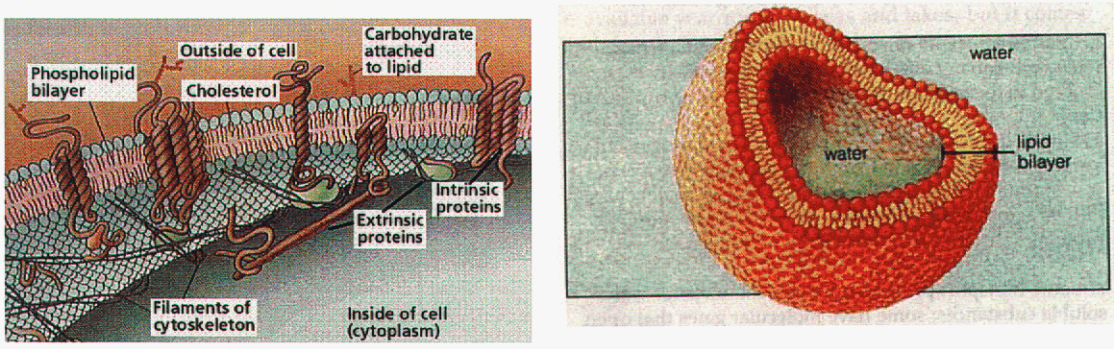


**Figure 3. Model of the lipid membrane of a cell (left, image from Purves, et al. Life: The Science of Biology, 4th ed., Sinauer Assoc.) and a cut away view of a lipid bilayer vesicle, or liposome (right) (from website: place.dawsoncollege.gc.ca/~rhanna/Membrane.htm).**

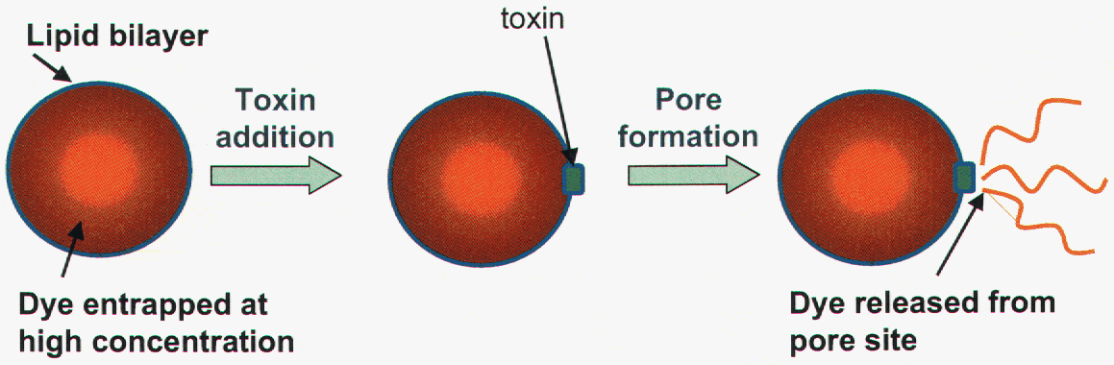


**Figure 4. Illustrated model of the liposome leakage study where toxin binding and pore formation leads to dye leakage and a subsequent increase in dye fluorescence.**

A model membrane was chosen based on numerous design constraints and experimental data that provided the essential traits of the cell membrane but yet offered stability as a single bilayer and was free of structural features that could hamper our molecular imaging efforts. The chosen membrane consists of three components: the ganglioside $G_{T1b}$, which is one of the known ligands of TetTx, and an equimolar concentration of DPPC and cholesterol to form a stable liquid ordered membrane phase. This phase is often found in lipid rafts of cell membranes. The molecular structures of the molecules can be found in Figure 5. Compositions of this lipid mixture readily formed large unilamellar liposomes via the extrusion method.

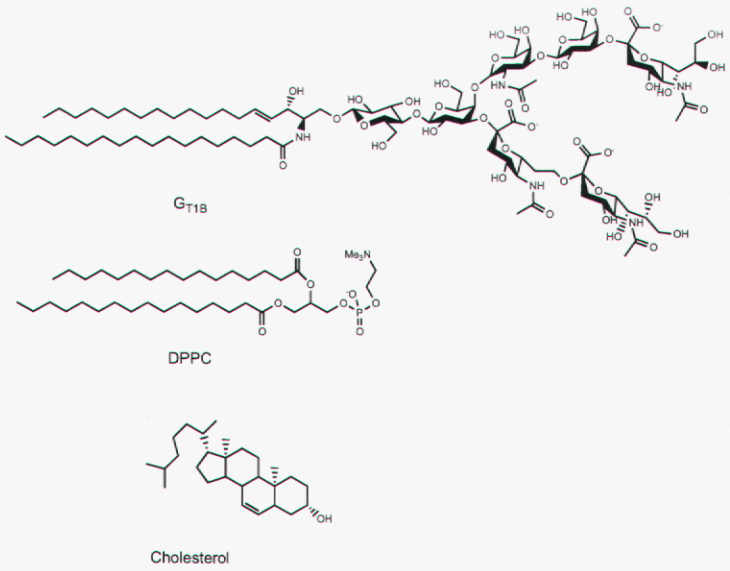


**Figure 5. Lipids used in the leakage study: $G_{T1b}$, DPPC, and cholesterol.**

Leakage studies were performed with Texas red as the encapsulated dye because of its fluorescence stability between pH 4 thru 7. At the entrapment concentration of 50 mM, the dye's fluorescence is quenched. The liposomes (100 nm diameter) were prepared by extrusion and isolated via gel permeation chromatography. The liposomes were placed in either pH 7 or pH 4 MES/HEPES/citrate buffer and their stability was evaluated at 37 °C by monitoring dye leakage through the increase of solution fluorescence over time.

The bilayers with and without $G_{T1b}$ had a background leakage of ca. 5% from entrapped Texas red over a period of 33 min (Figure 6). The control experiments that contained none of the ganglioside $G_{T1b}$ (i.e. the 50% DPPC/cholesterol bilayers) had a leakage of 3% at pH 7 over this time period while the same liposomes at pH 4 leaked about 5% of their entrapped dyes. Under the pH gradient the control liposomes also leaked about 5%. The $G_{T1b}$ containing liposomes all leaked the same amount of dye (6%) regardless of the pH conditions.

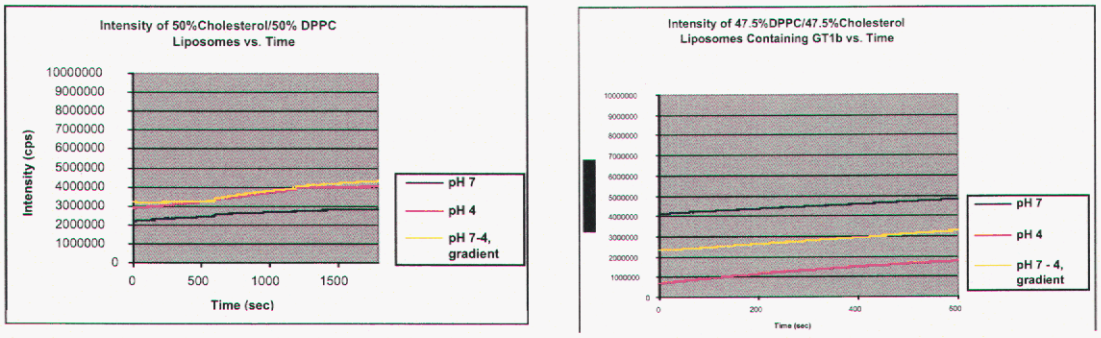


**Figure 6. Plot of fluorescence intensity of Texas red (excitation at 586 nm, emission monitored at 620 nm) as it leaks out of the control and $G_{T1b}$ containing liposomes at pH 7 and 4 and with the pH gradient from 7 to 4.**

Whole TetTx was added to solutions of the dye-entrapped liposomes yielding toxin concentrations of 8.3, 83, and 166 nM. Although all concentrations of toxin showed similar trends in liposome leakage, the data from 83 nM toxin showed the greatest effect between the various experiments. All data shown henceforth are from the experiments performed at 83 nM of toxin. The fluorescence intensity of the Texas red was recorded over time and the plots from the experiments at different pH are shown in Figure 7. The runs were interrupted every 10 minutes for a brief wavelength scan (590-650 nm) to verify that the emission shape did not change or shift. In the case of generating a pH gradient, a volume of 0.1N HCl was added after ~10 minutes of incubation time.

For control studies using 50% DPPC/cholesterol liposomes in the presence of TetTx. dye leakage was greatest under the pH gradient showing a release of 10% of total entrapped dye. Leakage from the liposomes under constant pH were considerably less with < 1% from that at pH 7, and 5% from pH 4. While the leakage at pH 4 can be attributed to background leakage, the leakage observed at pH 7 is considerably less than previously observed in the absence of TetTx. It is not understood at this time why this occurs.

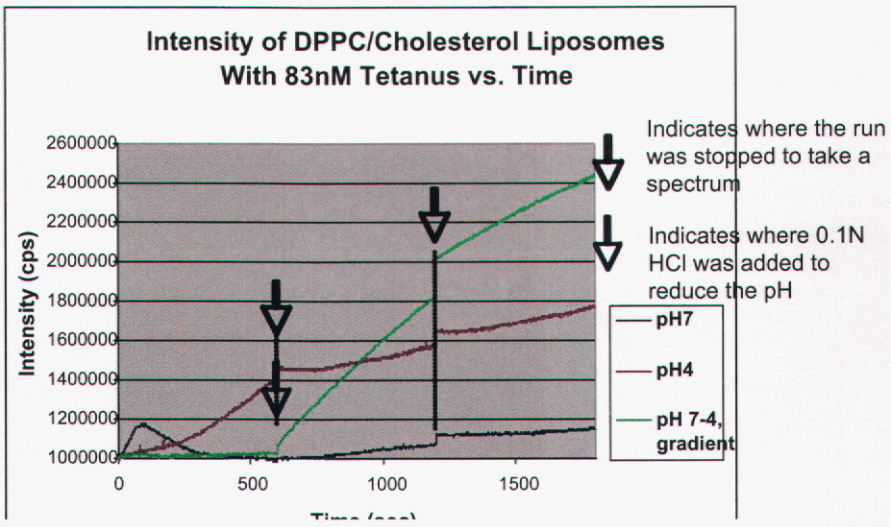


**Figure 7. Leakage of Texas red from 50% DPPC/cholesterol liposomes in the presence of tetanus toxin at constant pH of 7 and 4 and with the pH gradient from 7 to 4.**

For the $G_{T1b}$ containing liposomes (5% $G_{T1b}$/ 47.5% DPPC/ 47.5% cholesterol) in the presence of TetTx, the greatest amount of dye release also occurred under the pH gradient from 7 to 4 (Figure 8). In this case 35% of total entrapped was released over the 33 minutes of the experiment at a fairly linear rate. Under constant pH of 7, membrane leakage was considerably lower than with the pH gradient but still high with an observed loss of 21%. At constant pH 4 the dye leakage was only 8%, slightly higher than the background leakage.

These set of experiments verify the selectivity that the liposomes exhibit with whole tetanus toxin and its activation through a pH gradient, from neutral to acidic, as the toxin would experience in the endosome. Leakage is near background levels for the control experiments showing that TetTx targets membranes functionalized with $G_{T1b}$. With the $G_{T1b}$ containing liposomes the activity of the toxin was apparent at constant pH 7, but greatly elevated under the pH gradient. At constant pH 4, however, the pore activity was minimal producing a leakage only slightly above the background level. These results could be best explained by considering that the toxin recognizes and binds to cell surfaces at pH 7, and is activated to penetrate the membrane through a lowering of the solution pH. By merely binding to the membrane at pH 7, the toxin may perturb the model membrane through undefined insertion mechanisms resulting in a release of a portion of the liposome contents. At low pH, however, the toxin may acquire a conformation or surface charge that inhibits its affinity towards the $G_{T1b}$ and thus little leakage results from the toxin's presence.

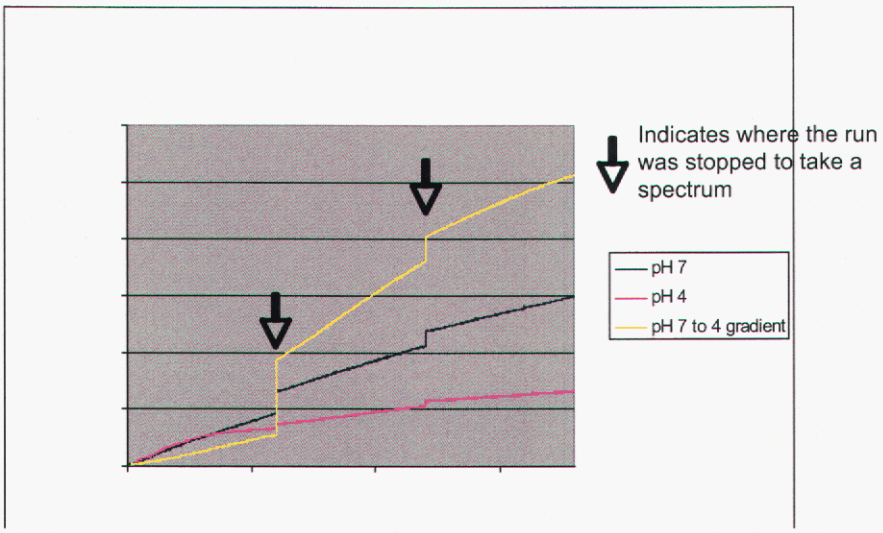


**Figure 8. Leakage of Texas red from 5% $G_{T1b}$/47.5% DPPC/47.5% cholesterol liposomes in the presence of tetanus toxin at constant pH of 7 and 4 and at with the pH gradient from 7 to 4.**

The leakage experiments provided the means to identify a lipid membrane composition with selective susceptibility to the binding and penetrating action of tetanus toxin. The mode of activity that the toxin takes at the molecular level, though, remains unclear. In forming the pore the toxin may act alone or in concert with others targeting specific features in the membrane. Conformational changes that occur as the bound toxin penetrates the membrane must be understood to provide further insights into biotoxin activity and the means of inhibition. Thus, imaging of the toxin-membrane interaction at the nanometer scale is imperative to provide a detailed understanding of the modus operandi of this deadly intruder.

## Scanning Probe Imaging of the C Fragment on Lipid Membrane

The first step towards understanding the molecular level interactions of TetTx on the lipid membrane is to study the binding domain. Tetanus toxin C fragment (Tet C) is widely believed to be the domain of the heavy chain responsible for the selective binding to cell surface ligands, in particular $G_{T1b}$. The fragment is reasonable large at 47,000 kD to provide adequate resolution of individual monomers with the AFM. AFM studies were conducted on supported lipid bilayers of a 10% $G_{T1b}$/45% DPOPC (dipalmitoleoyl-phosphatidylcholine)/45% DPPC fused to freshly cleaved mica surfaces.

To gauge the size and shape of Tet C on surfaces with the AFM, Tet C was adsorbed onto mica and imaged. Adsorption of Tet C was performed by adding approximately 150 μL of a 0.1 μM solution of the fragment in phosphate buffer solution at pH 7.4, into the solution cell of the AFM. After ~30 minutes of incubation at room temperature, tapping mode atomic force microscopy (TMAFM) imaging revealed small, randomly distributed aggregates having a height of ~3.5 nm and widths ranging between

20 - 40 nm, on the the mica surface (Figure 9). Comparison of the observed dimensions with the proposed Tet C crystal structure (and considering AFM tip convolution effects) indicates that Tet C absorbs to mica as both small aggregates and as single molecules. Electrostatic potential maps of the Tet C surface reveal a large area of negative charge (red area) opposite to the ganglioside binding region, which is an area of high positive charge (blue area) (Figure 9, right side). As both $GT_1B$ and mica are negatively charged at neutral pH, this suggests that Tet C interacts with the mica surface in an orientation similar to that with its receptor. This orientation is consistent with the structures observed by TMAFM.

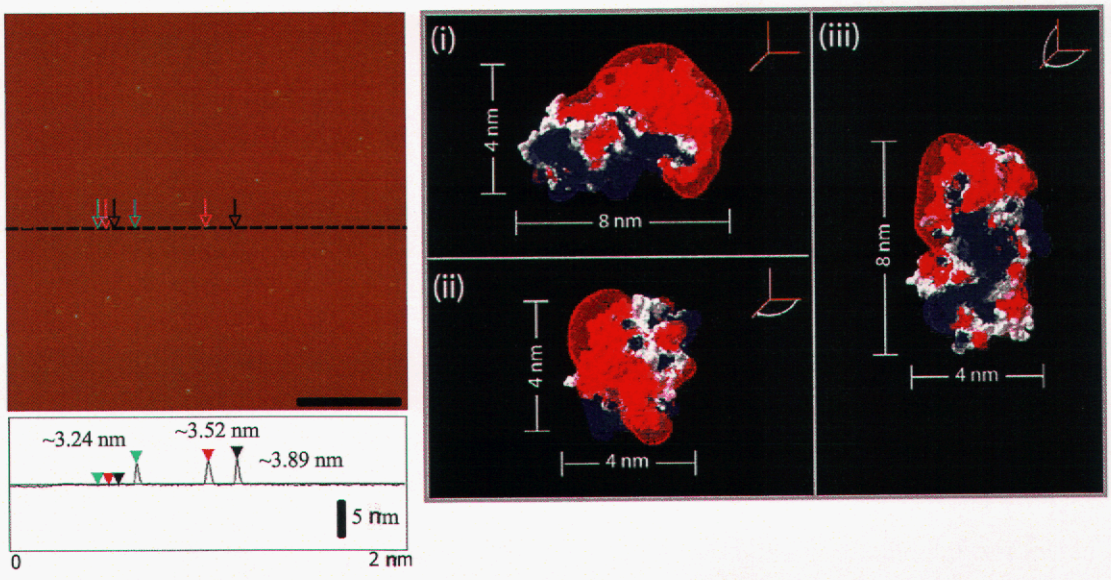


**Figure 9. AFM image of tetanus toxin C fragment on mica (left) and structural models prepared using the PDB model 1FV2 and the SwissPDB Viewer software package (GlaxoSmithKline) (right).**

Supported planar lipid bilayers (SPBs), containing equimolar amounts of DPPC and 1,2-dipalmitoleoyl-*sn*-glycero-3-phosphocholine (DPOPC) and 10 mole % $G_{T1b}$, were formed through the fusion of pre-formed unilamellar lipid vesicles on freshly cleaved mica in MES/HEPES/citrate buffer. SPBs are known to be separated from the underlying substrate by an ~1 nm fluid layer, thus allowing them to retain their semi-fluidic nature.

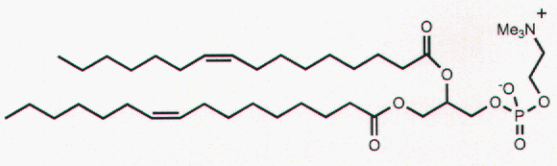


**Figure 10. Molecular structure of DPOPC.**

Figure 11 shows a schematic of the vesicle fusion process in the solution cell of the AFM and the resultant supported lipid bilayer on mica. Since the phase transition temperature of DPPC and DPOPC are so different, with $T_c$ = 41 °C for DPPC and $T_c$ < r.t. for DPOPC, it was expected that the two major lipid components of the membrane would phase separate into gel phase domains rich in DPPC and fluid phase regions rich in DPOPC. The AFM image of the bilayer shown in Figure 12a indeed finds that two distinct domains exist in the membrane defined by taller lipid structures of various shapes in a sea of shorter lipids. The taller domains extended ~1.5 nm above the shorter domains, corresponding to DPPC and DPOPC, respectively.

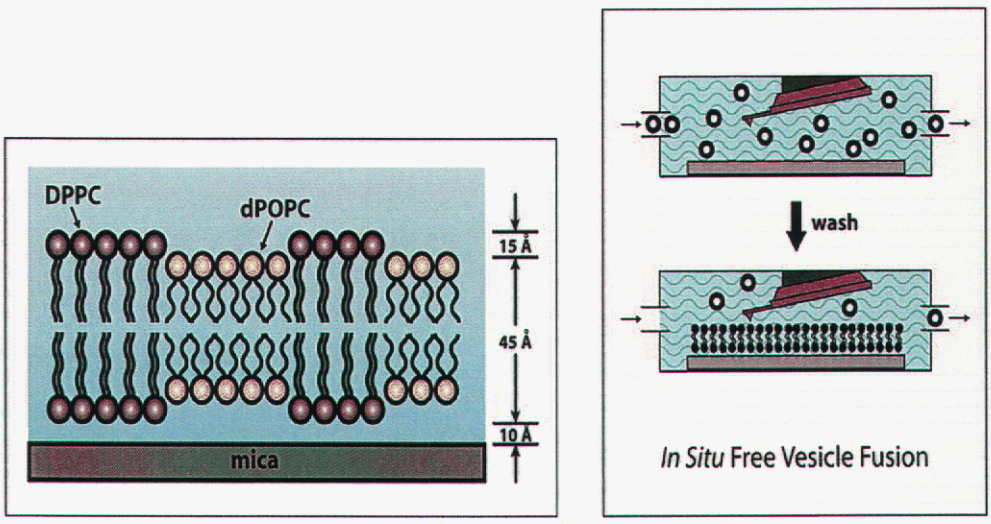


**Figure 11. Illustration of the DPOPC/DPPC supported lipid bilayer (left) and the vesicle fusion process on mica in the solution cell of the AFM (right).**

After ~2 hrs of exposure of the SPBs to a 0.2 μM solution of Tet C the AFM image (Figure 12b) shows that the protein preferentially associated with the fluid phase domains of DPOPC. Upon further incubation at room temperature for ~12 hrs, imaging of the same area revealed a dramatic change in bilayer morphology (Figure 12c). The membrane now had a single thickness of ~ 7 nm. While the DPPC domains remained relatively unchanged, the DPOPC domains grew in thickness and developed a granular texture populated with circular defects having diameters in the range of 40 - 80 nm. Figure 12d and 12e show that aggregates of Tet C associated with DPPC extended ~ 2 nm above the bilayer surface while those associated with DPOPC extended < 1 nm above the surface of the bilayer, suggesting at least partial insertion of Tet C within the fluid phase of the bilayer.

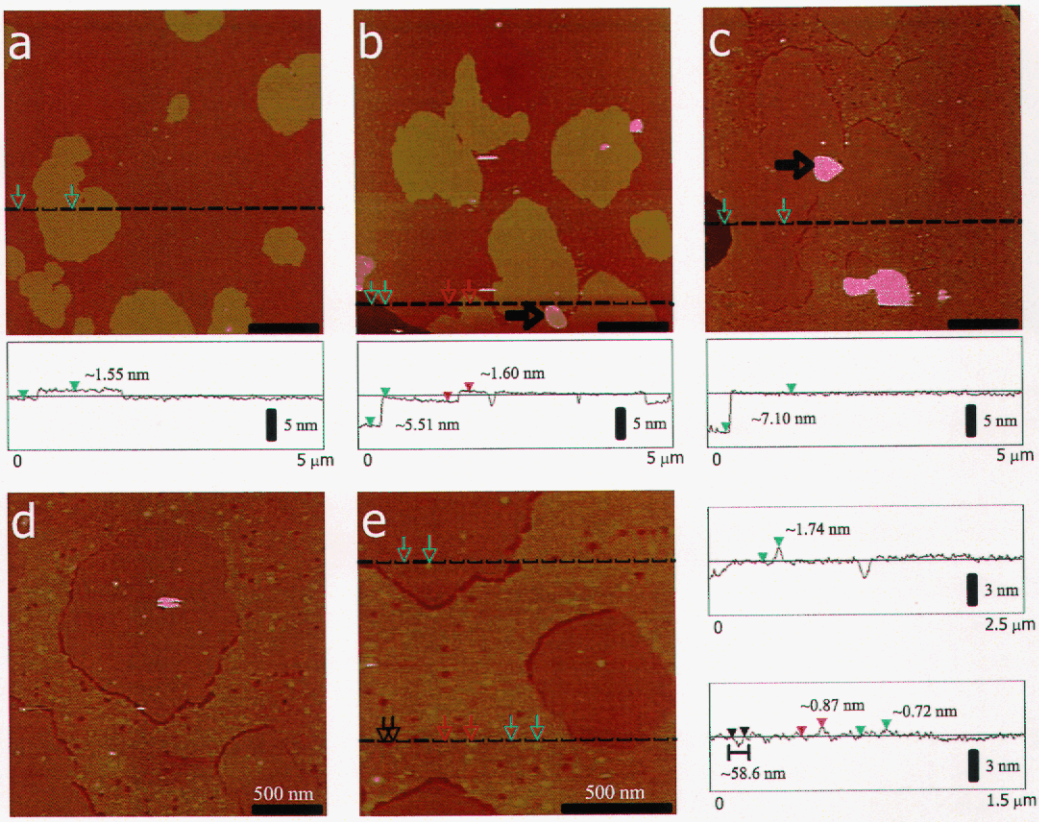


**Figure 12. AFM images with height profiles of the 10% $G_{T1b}$/45% DPOPC/45% DPPC bilayers on mica (a) before and (b) after ~2 hours and then (c – e) after ~12 hours of incubation with Tet C.**

A 3D AFM image of the 10 mol% $G_{T1b}$/45% DPOPC/45% DPPC lipid bilayer after ~12 hrs incubation with Tet C at pH 7.4 can be found in Figure 13. The 3D image clearly shows the granular appearance of the DPOPC rich areas populated by numerous pore-like defect structures. It is also apparent that far more Tet C associated with the fluid phase domains of DPOPC than the gel-like domains of DPPC. The DPPC domains, on the other hand, remained relatively unaltered after the addition of Tet C.

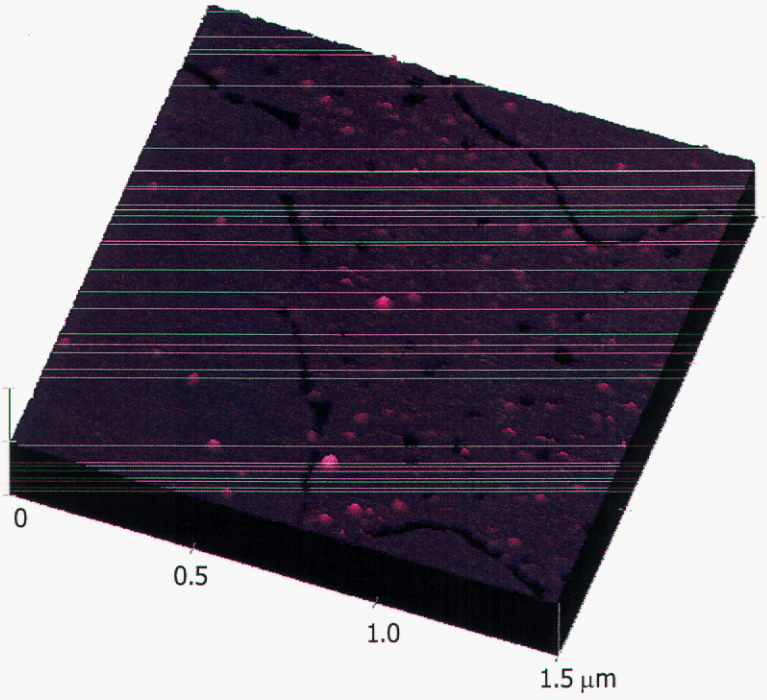


**Figure 13. 3D AFM image with of the 10% $G_{T1b}$/45% DPOPC/45% DPPC bilayers on mica following 12h incubation with tetanus toxin C fragment at pH 7.**

An experiment was also performed at low pH with Tet C to investigate the toxin's affinity to the membrane and correlate the findings with the results observed with the leakage studies. Figure 14 shows that after ~12 hours of incubation at pH 4.0, Tet C did not appear to associate with the surface of the membrane. This result strengthens the hypothesis that the toxin cannot recognize or bind to the membrane at low pH. Similarly, Tet C did not bind to lipid membranes that were void of $G_{T1b}$ at neutral pH (images not shown).

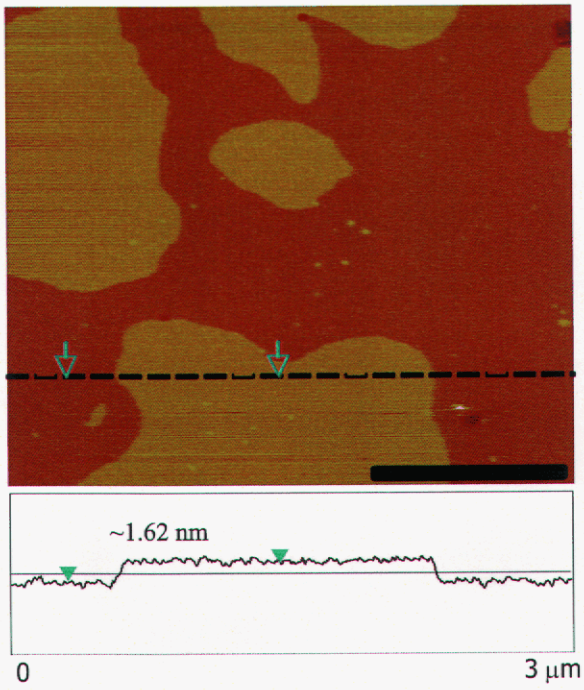


**Figure 14. AFM image with of the 10% $G_{T1b}$/45% DPOPC/45% DPPC bilayers on mica following 12h incubation with tetanus toxin C fragment at pH 4.**

## Conclusion

We have shown that whole Tetanus toxin selectively bound to $G_{T1b}$-laden lipid membranes and induced pore formation at neutral pH, while enhancement of pore activity occurred upon subsequent lowering of solution pH. In the absence of $G_{T1b}$, pore formation still appears to occur but at a markedly reduced level. *In situ* nanoscale imaging of supported lipid membranes showed that the pore formation was generated through the activity of the C fragment of the toxin alone. The C fragment was found to preferentially associate with the fluid phase of a two-phase lipid membrane. While this may indicate partitioning of $G_{T1b}$ within the fluid phase of the lipid bilayer, it may also simply reflect a greater degree of mobility of the receptors within the fluid matrix, and hence greater ease in adopting the correct binding conformation. Both the leakage and AFM imaging studies found that the binding and activity of the toxin on lipid membranes was poor if the complexation occurred at low pH or in the absence of $G_{T1b}$. Although the C fragment showed evidence of pore formation in biphasic membranes, further studies are being pursued with whole toxin on $G_{T1b}$/cholesterol/DPPC bilayers using the pH gradient at 37 °C to capture, as close as possible, the nanoscale details of toxin superstructure formation and pore generation in the membrane in a biologically relevant system.

## Experimental

**General**. All lipids were purchased from Avanti Polar Lipids (Alabaster, AL) and used as received. The sulforhodamine 100 (Texas Red) and Sephadex G-50 were purchased from Aldrich Chemical Company (Milwaukee, WI), the tetanus toxin C fragment and whole toxin (*Clostridium tetani*) were purchased from Calbiochem (La Jolla, CA), Triton X-100 was purchased from Sigma (St. Louis, MO). Aqueous solutions were prepared from water purified through a Barnstead Type D4700 NANOpure Analytical Deionization System with ORGANICfree cartridge registering an 18.0 MΩ-cm resistance. The aqueous buffer solution was prepared using 5 mM 4-morpholineethanesulfonic acid (MES), 5 mM 4-(2-hydroxyethyl)-1-piperazineethanesulfonic acid (HEPES), 5mM citric acid, and 150 mM NaCl, and the pH adjusted to the appropriate pH.

**Liposome leakage studies**

Lipid bilayer vesicles (50% cholesterol/DPPC and 47.5% cholesterol/47.5% DPPC/5% $G_{T1b}$) were prepared by extrusion in a pH 7.0 solution of 50 mM sulforhodamine using a Lipex Thermobarrel extruder (Northern Lipids, Inc., Vancouver, BC) with a 100 nm pore filter at 60 °C under high pressure argon gas. Vesicle diameters were measured using a DynaPro dynamic light scattering instrument (Protein Solutions, Lakewood, NJ) and confirmed at 100 ± 5 nm diameter. The dye entrapped liposomes were then separated from the non-entrapped dye using a Sephadex gel permeation chromatography column with MES/HEPES/citrate buffer. The osmolarity of the buffer, measured with a Fiske One-Ten Osmometer (Norwood, MA), was adjusted with NaCl to match the entrapped dye solution. The isolated liposomes fractions were combined and diluted five-fold for the leakage studies.

To quantify the amount of entrapped dye both sets of liposomes were lysed with Triton X-100 and the fluorescence intensity monitored before and after lysing using a SPEX Fluoromax II spectrophotometer (Edison, NY). The sample cell was jacketed at a temperature of 37°C. Lysing was executed at both pH 4 and 7.

Solutions of whole tetanus toxin were made using the 5 mM MES/HEPES/citrate buffer at pH 7. For the whole toxin, 25 μg of the toxin was dissolved in 100 μg of buffer to yield a concentration of 1.67 μM. All handling of the toxins were done in a laminar flow fume hood and the area work area was cleansed with a 5% bleach/water solution.

A three-by-three matrix of experiments was performed for each liposome composition. On one axis are the toxin concentrations of 8.3 nM, 83 nM, 166 nm, and on the other axis are experiments done at pH 7, 4, and a gradient from 7 to 4. Leakage data were first collected for the 50% cholesterol/DPPC liposome control on the fluorometer over a time period of 30 minutes ($\lambda_{ex}$ = 586 nm, $\lambda_{em}$ = 620 nm). Immediately following the end of the run a wavelength scan from 590-650nm was run to check that the wavelength peak had not shifting over the time course of the experiment. The matrix was then repeated for the 5% $G_{T1b}$/47.5% cholesterol/47.5% DPPC liposomes. The fluoroscence data were combined to show a representative plot of the intensity characteristics a function of the tetanus concentration and pH for each of the two sets of liposomes. All experiments were conducted at 37°C.

## *In situ* Tapping Mode Atomic Force Microscopy

**Liposome Preparation**: Equimolar quantities of 1,2-dipalmitoleoyl-sn-glycero-3-phosphatidylcholine (DPOPC) and DPPC, and where required, the appropriate amount of GT1B (10 mol%, 1 mol%), were dissolved in chloroform. The solvent was removed by evaporation under vacuum and the dried lipid films were rehydrated by the addition of 5 mM MES/HEPES/citrate buffer (150 mM NaCl, pH 7.4) to give a final lipid concentration of 2mM. Unilamellar vesicles were then formed by sonication in a heated water bath (~50°C) (Branson 200, Branson Ultrasonics Corp., Danbury, CT) until the solution became clear or only slightly hazy. The resulting liposomes were found to be ~145 nm in diameter by dynamic laser light scattering.

**Imaging**: Solution tapping mode AFM (TMAFM) images were acquired on a Digital Instruments Nanoscope IIIa Multimode SPM (Santa Barbara, CA), equipped with an 'E' scanner (13.6 μm x 13.6 μm maximum lateral scan area), using 120 μm DNP-S (Dimension silicon nitride probe-oxide-sharpened) V-shaped cantilevers installed in a combination contact/tapping mode liquid flow-cell sealed against a freshly cleaved mica substrate. All AFM imaging was conducted at ambient temperature. For Tet C studies on mica, ~150 μL of a 0.1 μM Tet C solution (10 mM PBS, 150 mM NaCl, pH 7.4) was applied to the mica surface. The fluid cell was flushed through with protein-free buffer after a 30 minute incubation period.

Supported planar lipid bilayers were formed in situ by injecting a ~200 μL liposome solution directly into the fluid cell and allowing them to adsorb to the mica surface for ~10 minutes. The fluid cell was then flushed with 10 mM $CaCl_2$ solution to facilitate fusion and incubated at room temperature. Once the bilayers were formed, calcium ions were removed by flushing the fluid cell with 10 mM EDTA solution. TMAFM imaging of the bilayer surface was conducted in 5 mM MES/HEPES/citrate buffer (pH 7.4). Approximately 300 μL of a 0.2 μM MES/HEPES/citrate solution (pH 7.4) of Tet C was injected directly into the fluid cell and imaging initiated after ~1 hr. In the case of experiments carried out at pH 4.0, bilayers were formed at pH 7.4 and the imaging fluid exchanged with MES/HEPES/citrate buffer (pH 4.0) before the addition of Tet C. For these studies, the 0.2 μM Tet C solution was also made up in MES/HEPES/citrate buffer (pH 4.0).

**Image Analysis**: Image analyses were conducted using the Digital Instruments Nanoscope software (version 4.42r9). Height images were low-pass filtered and plane-fit in the x-scan direction. Quantitative height measurements were determined by section analysis.

# References


i. Lebeda FJ, Singh BR. 1999. Membrane Channel Activity and Translocation of Tetanus and Botulinum Neurotoxins. J. Toxicol. - Toxin Reviews 18:45 - 76.

ii. Li L, Singh BR. 1999. Structure-Function Relationship of Clostridial Neurotoxins. J. Toxicol. - Toxin Reviews 18:95 - 112.

iii. Helting TB, Zwisler O. 1977. Structure of Tetanus Toxin. I. Breakdown of the Toxin Molecule and Discrimination between Polypeptide Fragments. J. Biol. Chem. 252:187 - 193.

iv. Robinson JP, Hash JH. 1982. A review of the molecular structure of tetanus toxin. Molec. Cell. Biochem. 48:33 - 44.

v. Schiavo G, Montecucco C. 1997. The Structure and Mode of Action of Botulinum and Tetanus Toxins. The Clostridia: Molecular Biology and Pathogenesis: Academic Press. p 295 - 322.

vi. Ginalski K, Venclovas C, Lesyng B, Fidelis K. 2000. Structure-based sequence alignment for the b-trefoil subdomain of the clostridial neurotoxin family provides residue level information about the putative ganglioside binding site. FEBS 482:119 - 124.

vii. Fu F-N, Busath DD, Singh BR. 2002. Spectroscopic analysis of low pH and lipid-induced structural changes in type A botulinum neurotoxin relevant to membrane channel formation and translocation. Biophys. Chem. 99:17 - 29.

viii. Li L, Singh BR. 2000. Spectroscopic Analysis of pH-Induced Changes in the Molecular Features of Type A Botulinum Neurotoxin Light Chain. Biochemistry 39:6466 - 6474.

ix. Gambale F, Montal M. 1988. Characterization of the channel properties of tetanus toxin in planar lipid bilayers. Biophys. J. 53:771 - 783.

x. New RRC. 1990. Liposomes. Rickwood D, Hames BD, editors. New York: Oxford University Press. 301 p.

# Distribution

| | | |
|---|---|---|
| 1 | MS1413 | A. L. Slade, 08331 |
| 1 | MS0856 | A. E. Schroeder, 14419 |
| 1 | MS9292 | J. S. Schoeniger, 08321 |
| 1 | MS1413 | D. Y. Sasaki, 08331 |
| 1 | MS9291 | L. Napolitano, 08320 |
| 1 | MS9292 | M. Young, 08321 |
| 1 | MS1413 | T. Michalske, 08300 |

1 C. M. Yip
University of Toronto
Institute of Biomaterials and Biomedical Engineering
Toronto, Ontario M5S 3G9
CANADA

| | | |
|---|---|---|
| 3 | MS9018 | Central Technical Files, 8945-1 |
| 1 | MS0899 | Technical Library, 9616 |
| 1 | MS9021 | Classification Office, 8511/Technical Library, MS 0899, 9616 |
| 1 | MS9021 | Classification Office, 8511 for DOE/OSTI |
| 1 | MS0323 | D. Chavez, LDRD Office, 1011 |